Hindawi
Geofluids
Volume 2022, Article ID 4294389, 14 pages
https://doi.org/10.1155/2022/4294389

Research Article

Analysis on Stress-Strain Model of Unsaturated Ice-Containing Soil

Qiang Han, Zhiguo Wang, Zhenchao Teng, Yunfeng Zhang, Meng Xue, and Xiaokai Qin

Heilongjiang Key Laboratory of Disaster Prevention, College of Civil and Architecture Engineering, Northeast Petroleum University, Daqing 163318, China

Correspondence should be addressed to Qiang Han; bruise@alumni.sjtu.edu.cn

Received 25 May 2022; Revised 5 July 2022; Accepted 3 August 2022; Published 13 August 2022

Academic Editor: Dongjiang Pan

The relationship between the stress-strain characteristics of ice-containing unsaturated soil and its various physical properties has important implications for the design and construction of transportation and building projects. The study also reveals the varying phases of the substance that can be deposited within the pore space. During winter, the freezing-thawing cycles affect the various media that can be deposited within the soil pore space, such as water and other water. The presence of water and others in the soil's pores can cause a freeze-thawing phenomenon and a significant change in the material's elastic modulus. This paper presents a method that uses the representative elementary volume (REV) model to perform a representative state variable analysis on an unsaturated ice-containing soil with porosity. The three stress-strain REV models that were developed for the study were designed to analyze the properties of an unsaturated ice-containing soil under freezing-thawing conditions. Then a comprehensive analysis of the soil's various components was performed. The effects of frozen soil on the change law of the relationship between different porous medium are studied. The study also explores the effects of the presence of porosity on the variation law of the frozen soil relationship between the stress-strain. The paper presents the study of the variation characteristics of the elastic modulus of permafrost soil. It also explores the various factors (porosity, moisture content, ice percentage, and tortuosity) that influence the stress-strain characteristics of unsaturated soil.

1. Introduction

Ice-containing unsaturated soil is a typical heterogeneous multiphase material composed of soil and mineral particles, glue icing, unfrozen water, water vapor, and gas. Due to the interaction between the various phases, the mechanical properties of permafrost are very complex. The importance of the soil's elastic modulus is acknowledged by the various fields that are involved in the study of this parameter. In cold environment, the presence of water and others in the soil's pores can cause a significant change in the material's elastic modulus. This is because the temperature and the inner conditions of the soil can affect the effects of the moisture content and ice percentage.

Frozen soil's mechanical properties can have a significant impact on the construction and design of cold area facilities. In particular, the presence of frozen soil can cause various freezing conditions, such as the emergence of ice mantle. Understanding the mechanical properties of frozen soil is very important for the development of the force field. The paper's main objective is to provide a practical understanding of the effects of frozen soil on the mechanical properties.

Tsytovich [1] studied the elastic modulus of frozen soil the first time, and the results indicated the elastic modulus is influenced by the temp, component, moisture content, and surrounding pressure, in which temperature has the largest influence. After that, Simonsen et al. [2] found that after a complete freezing-thaw cycling, the elastic modulus of frozen soil reduces. In addition, through test results, Burland [3] indicated that the secant modulus has a strong dependence on stress path in a small strain range, and the reason for the influence of elastic modulus on stress path is

raised through the corner concept of stress path. Besides, Yu et al. [4] put into effect field pressure meter experiment on the frozen soil and measured its pressure meter modulus and shear modulus, and also the prediction formula of mechanical properties influenced by temperature and moisture content was proposed. Further, according to the triaxial compression test on saturated frozen saline silty clay, Yang et al. [5] found that the underlying flexible modulus increments with the increment of salt substance and temperature.

Parameswaran and Jones [6] explored the initial tangential modulus of frozen Ottawa sandy soil under different surrounding pressures, and the results indicated that under the surrounding pressure range of 0.1-75 MPa, the initial tangential modulus locates between 1250 and 2000 MPa, and its value is smaller than that obtained by the uniaxial compression test of Parameswaran [7] under the same temperature condition. This is on the grounds that the ice crystal in frozen soil crushes and pressure melts under high surrounding pressure, which induces the reduction of initial tangential modulus of frozen soil. In addition, Bragg and Andersland [8] conducted a tandem uniaxial compression test on frozen sandy soil under various strain rates and temperatures. This research found that the initial tangential modulus changes in a power function relationship with the temperature, while it changes in a piecewise power function relationship with the variation of strain rate.

The review directed by Xu et al. [9] investigated the mechanical properties of frozen silty sand when it was desalted. They viewed that as the underlying typical and secant modulus of the desalted material increment with the rising temperature and the encompassing tension. Contrasted with the regular saline frozen soil, the desalted material's mechanical properties are higher.

Li et al. [10] concentrated on the relationship of dynamic flexible modulus and damping proportion of frozen sand with recurrence, restricting tension and dynamic strain. The outcomes found that the powerful flexible modulus of frozen sandy soil diminishes with the rising hub strain and increments with the rising recurrence, while the damping proportion expires with the rising recurrence. Furthermore, Christ and Park [11] investigated the variety of dynamic flexible modulus, dynamic shear modulus and Poisson's proportion of sandy soil and silty soil with negative temperature, and the outcomes demonstrated that the lower the temperature, the bigger the unique versatile modulus; besides, the dynamic elastic modulus of various soil is different under the same condition, and the sandy soil has the largest dynamic elastic modulus; the silty soil has the minimum value, while the silt ranges in the middle. Moreover, Ling et al. [12] played out a pair of low-temperature dynamic triaxial test on frozen soil under various temperatures, encompassing strains, and dampness contents and concentrated on the variety law of the most extreme powerful versatile modulus, dynamic flexible modulus proportion, and skeleton bend of frozen soil.

Li and Fan [13] concentrated on the qualities of frozen soil under unique burden through triaxial test and reach the accompanying inferences: the powerful flexible modulus increments with the temperature and the unique strain; the most extreme powerful shear modulus increments with the surrounding tension and increments with the heap vibration recurrence; under a similar temperature, the more prominent the water content, the heap recurrence, and the dynamic damping proportion. Under a similar test conditions, the dynamic damping proportion continuously diminishes with the diminishing temperature. Liu et al. [14] concentrated on the unique attributes of permafrost along the Qinghai-Tibet Railway by directing the three-pivot trial of permafrost. The aftereffects of the review uncovered that the greatest unique shear strength can increment with the temperature and the rising pressure adequacy. However, it decreases with the increasing vibration cycle and the circumference pressure.

Above researches mainly established analytical or numerical models by adopting experiments or the characteristics of soil porous structure. Bear [15] proposed the concept of REV for the first time when studying porous medium soil seepage, and it has been widely used in the field of geosoil porous medium transport such as soil physics [16, 17] and digital core [18, 19]. Usually, the porosity parameters are preferred for micro-microscale geotechnical media to investigate and determine their REV [20–22], which is also consistent with the porosity parameter constraints used when Bear [15] first proposed the REV concept. In this paper, the condition is considered when the pore water is subjected freeze-thawing, and the stress-strain model for frozen soil is constructed, along with the calculation formula of elastic modulus.

2. REV Portrayal Way for Frozen Soil

2.1. REV Portrayal and Feature Way for Porous Medium. In general, porous medium has a multiphase structure; therefore, a proper scale needs to be selected for description its property. Currently, the main methods used in the study are the description and analysis of the porosity relationship. The representative elementary volume (REV) model is the most commonly used way for this type of work [16–40].

The representative elementary volume (REV) is a scale, and the mechanical parameters of porous media change in volatility with the increasing volume of porous medium. At the point while the volume increments to a certain worth of V, the mechanical parameters no longer change with the volume, and V is called the representative elementary volume (REV) of the porous medium.

In general, the value of V is in the range of $V_{\min} < V < V_{\max}$. V should not be too small, since it contains only a small number of the particles, and V is not too large to reflect the inhomogeneities in the macroscopic distribution, as displayed in Figure 1.

The quantity of porosity that is obtained by averaging over the value of the microscopic void space indicator function is called the macroscopic quantity. If the value of the porosity is plotted at a fixed position, the medial volume domain of the material will be affected by the variance in its porosity. In other words, if the value of the void space indicator function is not constant, the medial volume will be affected by the large-scale inhomogeneity of the porosity.

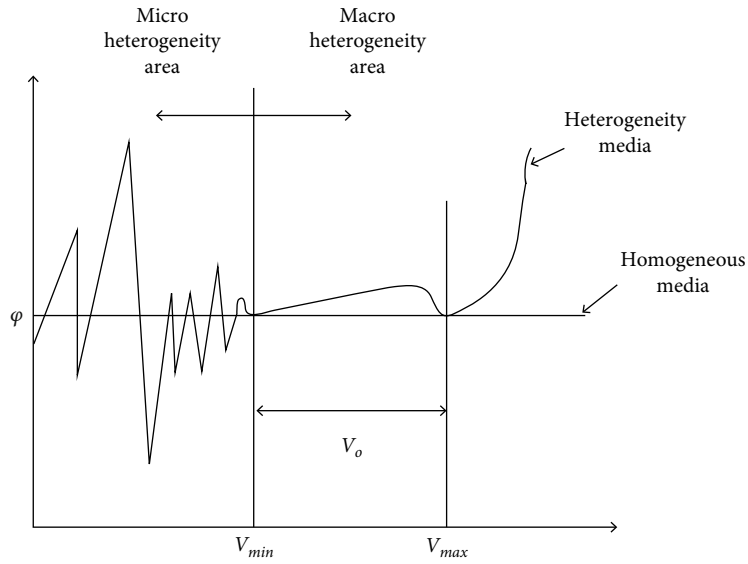

Figure 1: Porosity ϕ for various sizes of medial volumes.

The definition model shown in Figure 1 is an overall selection way for the study of the porosity relationship. In actual application process, as various porous media structures existed and the foundation for computation investigation and the application situations are likewise unique, the selection methods have different emphases.

2.2. REV Portrayal and Feature Way for Based on Porosity Concept. The soil porous media, similar to the general porous medium, are composed of the assembly of soil phase elements (spherical, flake, and acicular particles) and the interelement pores. The pore is filled with fluid, as a typical soil-fluid-gas three phase media, and the porosity is an important concept to describe the composition structure of porous media. Since the elastic modulus of the studied soil porous media is mainly affected by the composition structure, i.e., the porosity, therefore, this paper takes the porosity as the representative state variable and proposes the selection method for volume-weighted medial REV.

The porosity can be computed as a single continuum by taking into account the state variable of the media at any point in its continuous medium. The porosity can be computed as a single continuum by taking into account the state variable of the media at any point in its continuous medium, as displayed in Figure 2.

If the statistical medial state variable is the continuous function of the center point and the spatial coordinates of the selected volume, the representative elementary volume of the corresponding state variable is shown.

As displayed in Figure 2, this hypothesis considers that the unsaturated ice-containing soil has a geometrical zone Ω (REV zone), and it is divided into soil matrix zone Ω_S, water system zone Ω_W, ice system zone Ω_I, and air zone Ω_A [41].

If point x is a casual point in the unsaturated ice-containing soil's geometric zone Ω, the media zone taking point x as its geometric center is $\Omega(x)$, and its epitaxial quantity is $E(x)$.

When the epitaxial quantity in zone $\Omega_n(x)$ is $E_n(x)$, $F(x)$ is the inner parameters (structure, seepage, and pressure) in the macroscale of the epitaxial quantity of point x.

$$\begin{aligned} \Omega &= \sum_n \Omega_n,\ n \in \{S, W, I, A\}, \\ \Omega_n(x) &= \Omega(x) \cap \Omega_n,\ n \in \{S, W, I, A\}, \\ E(x) &= \sum_n E_n(x), \end{aligned} \tag{1}$$

$$F_n(x) = \lim_{V_0 \longrightarrow V} \frac{E_n(x)}{V_0}, \tag{2}$$

$$F_n(x) = \lim_{y \longrightarrow x} F_n(y),\ y \in \{\Omega(x)\}. \tag{3}$$

The selection of the media zone $\Omega(x)$ that meets the conditions specified in Equations (2) and (3) will result in the corresponding V as the unsaturated ice-containing soil's REV. In this paper, the analysis of soil porous media should select the REV in strain process (i.e., the volume-weighted medial REV), and the method is shown above.

3. Stress-Strain Model of Unsaturated Ice-Containing Soil

Because of the varying stress distribution inside the soil, it is difficult to describe the interior structure and composition of the material. The elastic modulus of a soil can be affected by its structure and composition. This is why it is important to conduct a comprehensive analysis of the stress transmission process. The authors performed a comprehensive analysis of the various factors that affect the elastic modulus of unsaturated soil. They created a model that takes into account the

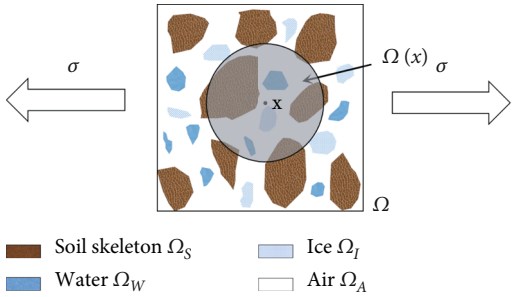

Figure 2: The medial volume centered on point x in the porous medium.

multiple parameters that affect the material's internal structure and composition. A computational formula was then developed for every model.

3.1. Simple Weighted Medial Volume REV Model. The simple weighted medial volume REV model is a model which could only be used for brief analysis when the internal and structural parameters of the characterization element are few. In most conditions, only an approximate range of porosity can be obtained for porous media, and the characterization parameters or internal structure are unknown, as shown in Figure 3.

As shown in Figure 3, when the element body is a one-dimensional structure, there is

$$\phi = \frac{x}{l}, \tag{4}$$

where ϕ is the porosity, x is the pore longness of the element body, and l is the element longness.

When the unit length is l, there is

$$\phi = x. \tag{5}$$

As shown in Figure 3, when the characterization element is a two-dimensional structure, the cross-section of pore is $x \times x$, and the cross-section of element body is $l \times l$. Based on the definition of porosity, the relationship between ϕ and x is

$$\phi = \frac{x^2}{l^2}. \tag{6}$$

When the unit length is l, there is

$$x = \sqrt{\phi}. \tag{7}$$

For the simple weighted medial volume REV model in Figure 3, on account of the connection between stress direction and pore location, the stress-strain model of soil porous media can be expressed as simple tandem (perpendicular) model and simple multipled (parallel) model.

The simple tandem (perpendicular) model is shown in Figure 4. At this time, the channel of the characterization

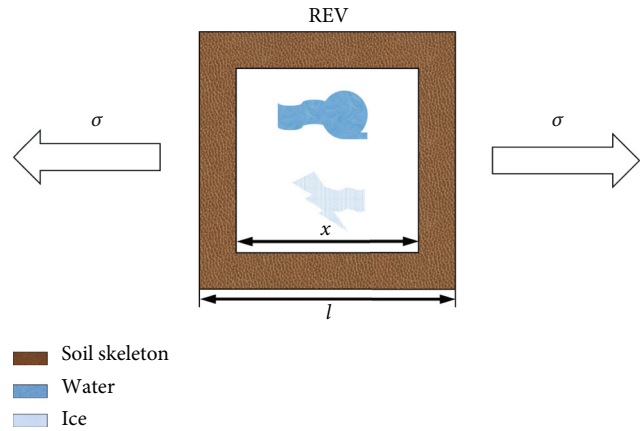

Figure 3: Simple weighted medial volume REV model.

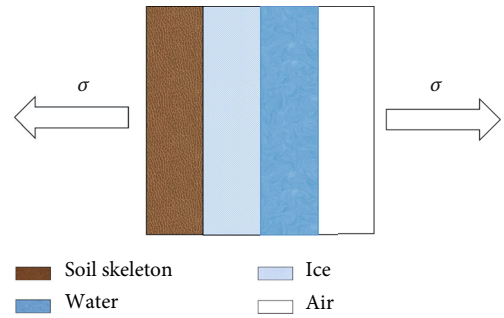

Figure 4: The simple tandem (perpendicular) model.

element is arranged perpendicularly in the soil's porosity medium, which is perpendicular to its stress direction.

For the model in Figure 4, L_g and L_k are the skeleton length and of characterization element, respectively.

According to the theory of mesomechanics of composite materials [42] and the Reuss tandem model [43], combined with the composition and mechanical characteristics of the frozen soil, the permafrost is regarded as a parallel isotropic solid medium composed of ice crystals, unfrozen water, air, and dry hard solid soil. According to the deformation coordination condition, typical microelementary volume of monolayer composites was used as the study subjects, and the elastic modulus of the isotropic surface of the frozen soil was deduced, respectively, as follows.

For the model in Figure 4, when analyzing stress and strain, this model can be expressed as the type of tandem spring system, as shown in Figure 5.

Here, the elastic modulus E_{air} [44] of ideal gas spring is introduced as the product of 1 atmospheric pressure P (kPa) and air compression coefficient Z (dimension of 1), that is

$$E_{air} = P \times Z = 101.325\text{kPa} \times 1 = 101.325\text{kPa} = 0.101325\text{MPa}. \tag{8}$$

For the system in Figure 5, E_s is the elastic modulus of soil skeleton, E_i is the elastic modulus of solid ice, and E_w is the elastic modulus of liquid water.

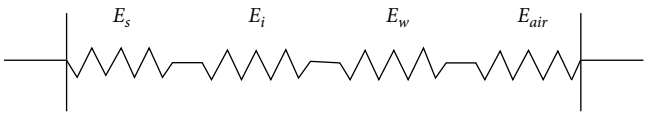

Figure 5: Analysis of tandem spring system.

Under 1D structure, based on Equation (5), there is

$$L_{k1} = x = \phi, \tag{9}$$

$$L_{g1} = 1 - x = 1 - \phi. \tag{10}$$

Under a 2D structure, based on Equation (7), there is

$$L_{k2} = x = \sqrt{\phi}, \tag{11}$$

$$L_{g2} = 1 - x = 1 - \sqrt{\phi}. \tag{12}$$

When analyzing stress and strain, the model can be expressed as the tandem type of several springs.

That is, the elastic modulus E_c by the simple tandem (perpendicular) model is

$$\frac{1}{E_c} = \frac{L_{g2}}{E_s} + \frac{L_{k2}}{E_{kc}}, \tag{13}$$

where E_{kc} is the internal tandem elastic modulus of pore.

Substitute Equations (11) and (12) into Equation (13), there is

$$\frac{1}{E_c} = \frac{\left(1 - \sqrt{\phi}\right)}{E_s} + \frac{\sqrt{\phi}}{E_{kc}}. \tag{14}$$

The solid ice, liquid water, and air contained in the pores can also be connected in tandem, and the obtained elastic modulus E_{kc} in tandem inside pore is

$$\frac{1}{E_{kc}} = \frac{1 - \alpha - \beta}{E_{air}} + \frac{\alpha}{E_i} + \frac{\beta}{E_w}, \tag{15}$$

where β is the moisture content, i.e., the volume ratio of liquid water in pores, and α is the ice percentage, i.e., the volume ratio of ice crystal in pores.

Substitute Equation (15) into Equation (14); we can obtain:

$$E_c = \frac{E_s E_{air} E_i E_w}{\left(1 - \sqrt{\phi}\right) E_{air} E_i E_w + E_s \sqrt{\phi}[(1 - \alpha - \beta) E_i E_w + \alpha E_{air} E_w + \beta E_{air} E_i]}. \tag{16}$$

Equation (16) is the calculation formula of elastic modulus by the simple tandem (perpendicular) model.

Figure 6 shows the multipled (parallel) model, which shows the channel of the characterization element in the soil's porosity medium being multipled to its components in the pores.

For the model in Figure 6, according to the theory of mesomechanics of composite materials [42] and Voigt multipled model [45], when analyzing stress and strain, this model can be expressed as the type of multipled spring system, as shown in Figure 7.

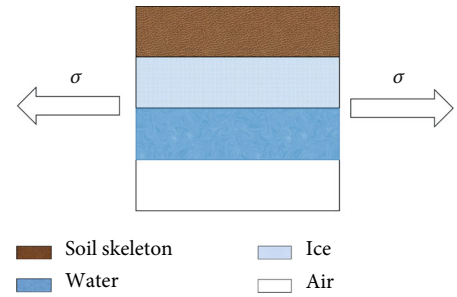

Figure 6: The multipled (parallel) model.

That is, the elastic modulus E_b by the simple multipled (parallel) model is

$$E_b = L_{g2} E_s + L_{k2} E_{kb}, \tag{17}$$

where E_{kb} is the internal multipled elastic modulus of pore.

Substitute Equations (11) and (12) into Equation (17); the following formula can be obtained:

$$E_b = \left(1 - \sqrt{\phi}\right) E_s + \sqrt{\phi} E_{kb}. \tag{18}$$

The solid ice, liquid water, and air contained in the pores can also be connected in multipled, and the obtained elastic modulus E_{kb} in multipled inside pore is

$$E_{kb} = (1 - \alpha - \beta) E_{air} + \alpha E_i + \beta E_w. \tag{19}$$

Substitute Equation (19) into Equation (18); the following equation can be deduced:

$$E_b = \left(1 - \sqrt{\phi}\right) E_s + \sqrt{\phi}[(1 - \alpha - \beta) E_{air} + \alpha E_i + \beta E_w]. \tag{20}$$

Equation (20) is the simple multipled model for calculating elastic modulus.

3.2. Fine Weighted Medial Volume REV Model. The fine weighted medial volume REV model refers to the condition when the basic and parameters and structure of the representative element in the soil porous media are basically known, as shown in Figure 8.

For Figure 8, the stress transmission process is calculated based on volume-weighted medial REV model, which thinks about the pore shape and channel distribution characteristics.

For consideration of pore curvature, the tortuosity τ_i is introduced, as the definition of

$$\tau_i = \frac{L_r}{L}, \tag{21}$$

where L_r is the genuine longness of the curved stoma access and L is the straight line longness connecting both ends of curved pore access.

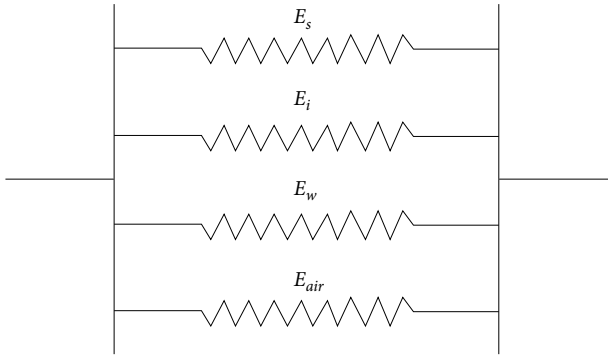

Figure 7: Analysis of multipled spring system.

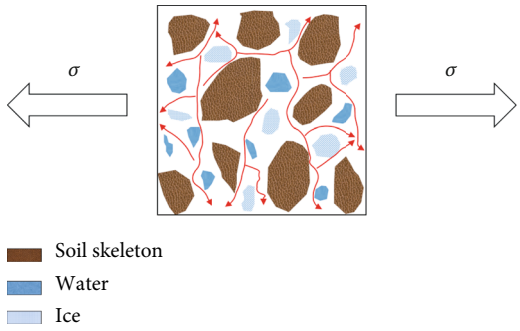

Figure 8: Fine weighted medial volume REV model.

Tortuosity is a parameter characterizing the curvature of pore access in the representative element, and the average tortuosity τ is

$$\tau = \sum_{i=1}^{N} \frac{\tau_i}{N}, \tag{22}$$

where N is the complete number of stoma accesses in the element.

Introduce the stoma access distribution parameter η, which is defined as the ratio of the number of tandem channels to the total number of channels in the representative element, that is

$$\eta = \frac{N_c}{N} \times 100\%, \tag{23}$$

where N_c is the quantity of pore accesses in tandem.

For the fine REV model in Figure 8, the elastic modulus should take into consideration of the tortuosity, stoma access distribution parameter, and elastic modulus of tandem and multipled models, that is

$$E_x = \tau[(1-\eta)E_b + \eta E_c]. \tag{24}$$

Substitute Equations (16) and (20) into Equation (24); the accompanying equation can be gotten:

$$E_x = \tau(1-\eta)\left\{\left(1-\sqrt{\phi}\right)E_s + \sqrt{\phi}[(1-\alpha-\beta)E_{air} + \alpha E_i + \beta E_w]\right\} + \frac{\tau\eta E_s E_{air} E_i E_w}{\left(1-\sqrt{\phi}\right)E_{air}E_i E_w + E_s\sqrt{\phi}[(1-\alpha-\beta)E_i E_w + \alpha E_{air}E_w + \beta E_{air}E_i]}. \tag{25}$$

Equation (25) is the elastic modulus calculation formula of fine weighted medial volume REV model.

3.3. Macro-Stress-Strain Analysis Model for Unsaturated Ice-Containing Soil. The stress-strain analysis model for macro-unsaturated ice-containing soil is based on the above simple and fine weighted medial volume REV models, as shown in Figure 9. The detailed analysis process is to divide the actual macrounsaturated ice-containing soil into $m \times n$ REV elements.

When adopting Figure 9 to analyze stress and strain, according to different stress transmission paths, the comprehensive model for stress transmission in soil porous media can be divided into the tandem-multipled model and the multipled-tandem model.

In the tandem-multipled model, n lines of spring are connected in tandem first, and they are treated as a whole; then m columns of spring are connected in multipled. The elastic modulus E_{gc-m} obtained by the tandem-multipled model is

$$E_{gc-m} = \frac{1}{m}\sum_{n=1}^{m} E_{gc-n}, \tag{26}$$

where E_{gc-n} is the elastic modulus after connecting n lines of spring.

After connecting n columns of spring in tandem, the following formula is obtained:

$$E_{gc-n} = \frac{E_{kc}E_s}{\sqrt{\phi_n}E_{kc} + \left(1-\sqrt{\phi_n}\right)E_s}, \tag{27}$$

where ϕ_n is the porosity of the nth colomn.

Substitute Equations (15) and (27) into Equation (26); the accompanying equation can be gotten:

$$E_{gc-m} = \frac{1}{m}\sum_{n=1}^{m} \times \frac{E_s E_{air} E_i E_w}{\left(1-\sqrt{\phi_n}\right)E_{air}E_i E_w + E_s\sqrt{\phi_n}[(1-\alpha-\beta)E_i E_w + \alpha E_{air}E_w + \beta E_{air}E_i]}. \tag{28}$$

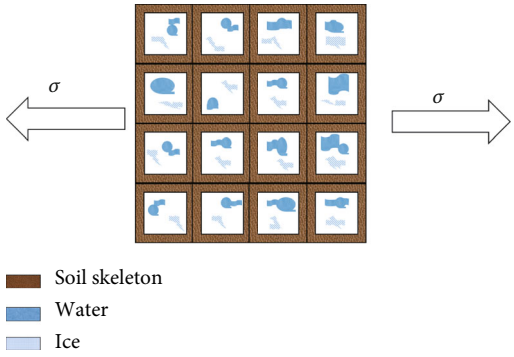

FIGURE 9: The stress-strain analysis model for macrounsaturated ice-containing soil.

Equation (28) is the tandem-multipled calculation formula for elastic modulus.

In the multipled-tandem model, m lines of spring are multipled first, and they are treated as a whole; then n columns of spring are connected in tandem. The elastic modulus E_{gb-n} obtained by the multipled-tandem model is

$$\frac{1}{E_{gb-n}} = \frac{1}{n}\sum_{m=1}^{n}\frac{1}{E_{gb-m}}, \tag{29}$$

where E_{gb-m} is the elastic modulus after m lines of spring are multipled.

When m lines of springs are multipled, we can deduce:

$$\frac{1}{E_{gb-m}} = \frac{1}{\sqrt{\phi_m}E_{kb} + \left(1-\sqrt{\phi_m}\right)E_s}, \tag{30}$$

where φ_m is the porosity in the mth line.

Substitute Equations (19) and (30) into Equation (29); the accompanying equation can be gotten:

$$\frac{1}{E_{gb-n}} = \frac{1}{n}\sum_{m=1}^{n}\times\frac{1}{\sqrt{\phi_m}[(1-\alpha-\beta)E_{air}+\alpha E_i+\beta E_w]+\left(1-\sqrt{\phi_m}\right)E_s}. \tag{31}$$

Equation (31) is the multipled-tandem calculation formula for elastic modulus.

4. Model Verify and Contrast of Numerical Calculation

4.1. Model Verify Way. The modulus of frozen soil has two determination ways:

(1) $\sigma-\varepsilon$ expressed as the slope of the line connecting the point on the curve $\varepsilon = 0.2\%$ is corresponding to the strain to the origin of the coordinates

(2) Based on the test data of uniaxial compressive strength, take the ratio of 1/2 of the instantaneous uniaxial compressive strength to its corresponding strain value:

$$E = \frac{\sigma_s}{\varepsilon_{1/2}}, \tag{32}$$

where E is the modulus of elasticity of the specimen, σ_s is the instantaneous uniaxial compressive strength of the specimen, and $\varepsilon_{1/2}$ is the strain corresponding to half of the instantaneous uniaxial compressive strength value of the specimen (%).

4.2. Model Verification. The choice of the latter representation method was taken into account when it came to the selection of the model's elastic modulus value. In order to test the model's correctness, Jiang [46] conducted an experiment that was conducted under the atmospheric pressure of 101.325 kPa. The data collected during the experiment were used to validate the model and the correctness of its design. Table 1 shows the various media and structural parameters [47, 48] that were involved in the study.

The macro-stress-strain analysis model is the most reasonable stress conduction model to the circumstance in the real world in the models, which is contrasted to experimental data, as shown in Figure 10.

As can be seen from Figure 10, both the experimental and calculated values show an increasing trend as the volumetric moisture content increases.

The calculated values of the macro-stress-strain analysis model established in this paper exhibited a maximum bias of 9.636% and a minimum bias of 0.069% compared with the experimental values. The permafrost modulus of elasticity calculated by the model proposed in this paper agrees well with the actual one. The results of the test results exhibited in Figure 10 differ from the simulated results due to the different properties of the soil's porosity and components. The paper also shows that the proposed stress-strain analysis model is not able to provide the most accurate simulation of the situation due to the heterogeneity of the media's properties. Meanwhile, the simple weighted medial volume REV model and the fine weighted medial volume REV model are also verified in this paper, which is similar to the macro-stress-strain analysis model, and will not be repeated in this section.

4.3. Engineering Application. Large-scale development and utilization of underground space have become an important means and development trend to expand the scope of human survival, and the artificial formation freezing method is increasingly used in underground engineering construction. The maintenance structure of artificial frozen soil wall is highly adaptable to complex hydrological and geological conditions, and the freezing construction methods are flexible and in various forms. In recent years, much attention in underground engineering construction, especially in the soft water-containing strata construction, is irreplaceable. And the study of elastic modulus in unsaturated ice-containing soil has an important influence in these projects.

Although the artificial freezing method has been widely used in the perpendicular well drilling and formation reinforcement, with the increase of the freezing depth of the perpendicular well and the thickness of the alluvial layer, the

Table 1: The soil structural parameters and media elastic modulus parameters in experiment.

Structural properties parameters		Medium elastic modulus	
Porosity	0.5	Media	Elastic modulus, MPa
Moisture content	0.16~0.26	Silty clay	12
Ice percentage	0.12	Ice	6820
Tortuosity	1.3	Air	0.101325
Stoma access composition parameter	0.83	Water	1980

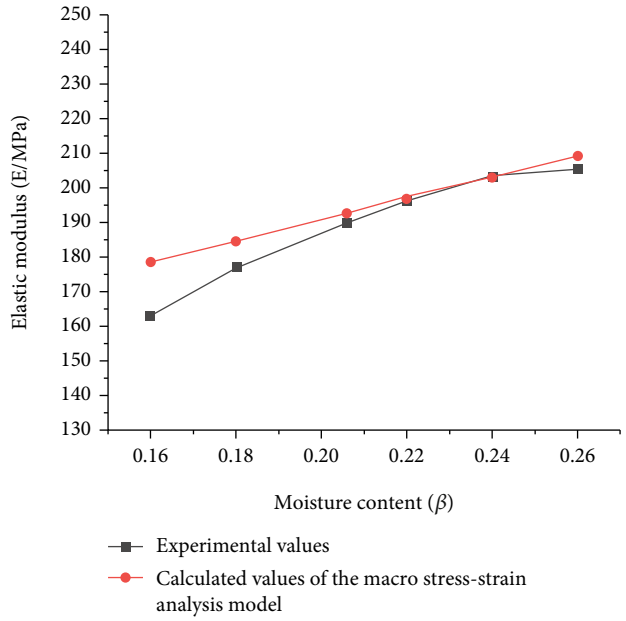

Figure 10: Connection among calculated and experimental values of the macro-stress-strain analysis model.

problems encountered in the freezing project have gradually become prominent. The toughest problem of the deep surface soil layer is how to ensure the strength and stability of the freezing wall and reduce the deformation of the freezing wall as far as possible, which plays a very important role in the fracture of the freezing tube. The elastic modulus of frozen soil is one of the main indexes of the mechanical properties of frozen soil and also an important parameter for freezing wall design. The elastic modulus was calculated by conducting the uniaxial unlimited compressive strength test. To study the influence of the elastic modulus of frozen soil affected by porosity, moisture content, and dry density and to explore the primary and secondary relationship of the influencing factors, this paper provides some basis for freezing method construction and theoretical research.

4.4. Numerical Calculation and Analysis. Accepting sandy soil as a model, and based on the established model and deduced formula, the influence of various parameters (porosity, moisture content, ice percentage, and tortuosity) on elastic modulus is analyzed through numerical calculation. The correlation coefficients are kept in Table 2.

Table 2: Elastic modulus of medium.

Standard atmospheric pressure 101.325 kPa, temperature 0°C	
Medium	Elastic modulus, MPa
Sandy soil	35
Ice	3200
Ideal gas spring	0.101325
Liquid water	2180

4.4.1. Elastic Modulus Calculation by Simple Weighted Medial Volume REV Model. Based on Equations (16) and (20), the elastic modulus is numerically calculated by simple weighted medial volume REV model.

Under the moisture content of $\beta = 0.3$ and ice percentage α of 0.1, 0.3, and 0.5, the changes of elastic modulus E of the tandem model with the porosity ϕ are displayed in Figure 11(a), and the changes of the elastic modulus E of the multipled model with the porosity ϕ are displayed in Figure 11(b). From this figure, it tends to be seen that, when the ice percentage is constant, the elastic modulus obtained by tandem model decreases with the increasing porosity, while that obtained by multipled model increases with the increasing porosity. Besides, when the porosity is constant, the elastic modulus obtained by these two models both increases with the increasing ice percentage.

Under the ice percentage of $\alpha = 0.3$ and moisture content β of 0.1, 0.3, and 0.5, the changes of elastic modulus E of the tandem model with the porosity ϕ are displayed in Figure 12(a), and the changes of elastic modulus E of the multipled model with the porosity ϕ are displayed in Figure 12(b). From this figure, it tends to be seen that, when the moisture content is constant, the elastic modulus obtained by tandem model decreases with the increasing porosity, while that obtained by the multipled model increases with the increasing porosity. Besides, when the porosity is constant, the elastic modulus obtained by these two models both increases with the increasing moisture content.

4.4.2. Elastic Modulus Calculation by Fine Weighted Medial Volume REV Model. Based on Equation (25), the elastic modulus is numerically calculated by fine weighted medial volume REV model.

Under the porosity of $\phi = 0.5$, moisture content of $\beta = 0.3$, ice percentage of $\alpha = 0.3$, the variation of elastic modulus E with tortuosity τ is plotted in Figure 13 with the stoma access distribution parameter η of 0.1, 0.3, and 0.5,

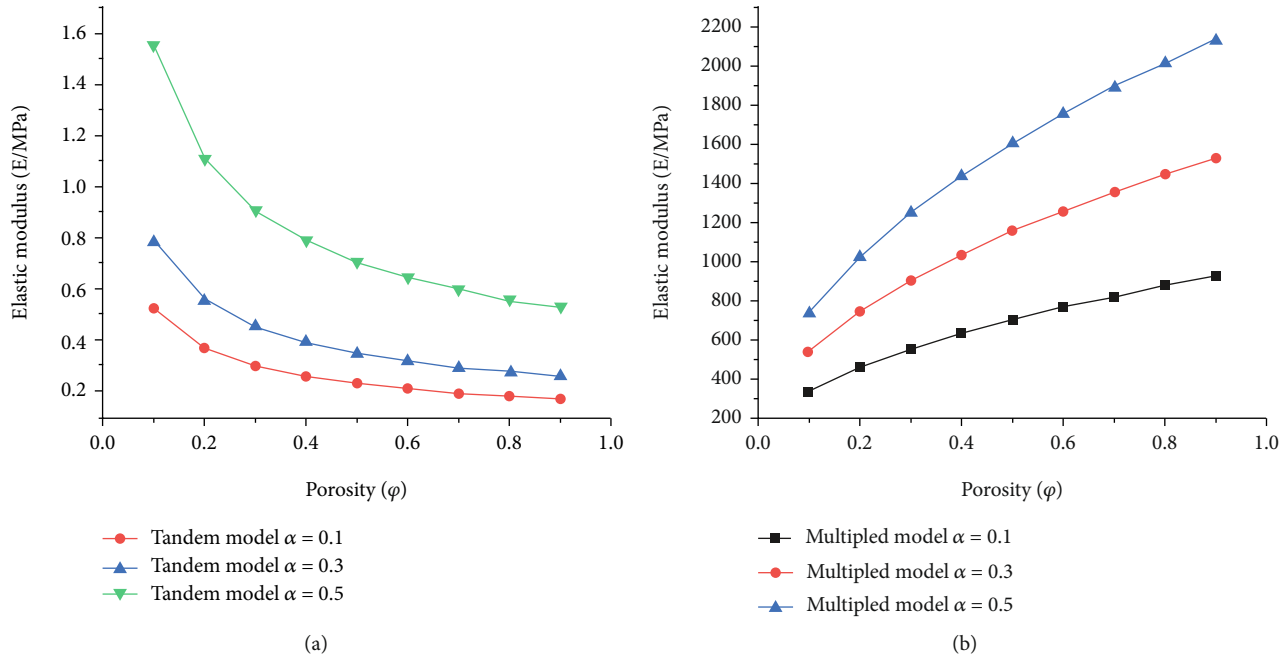

Figure 11: Relationship of elastic modulus E and porosity ϕ in simple weighted medial volume REV model under a different ice percentage α.

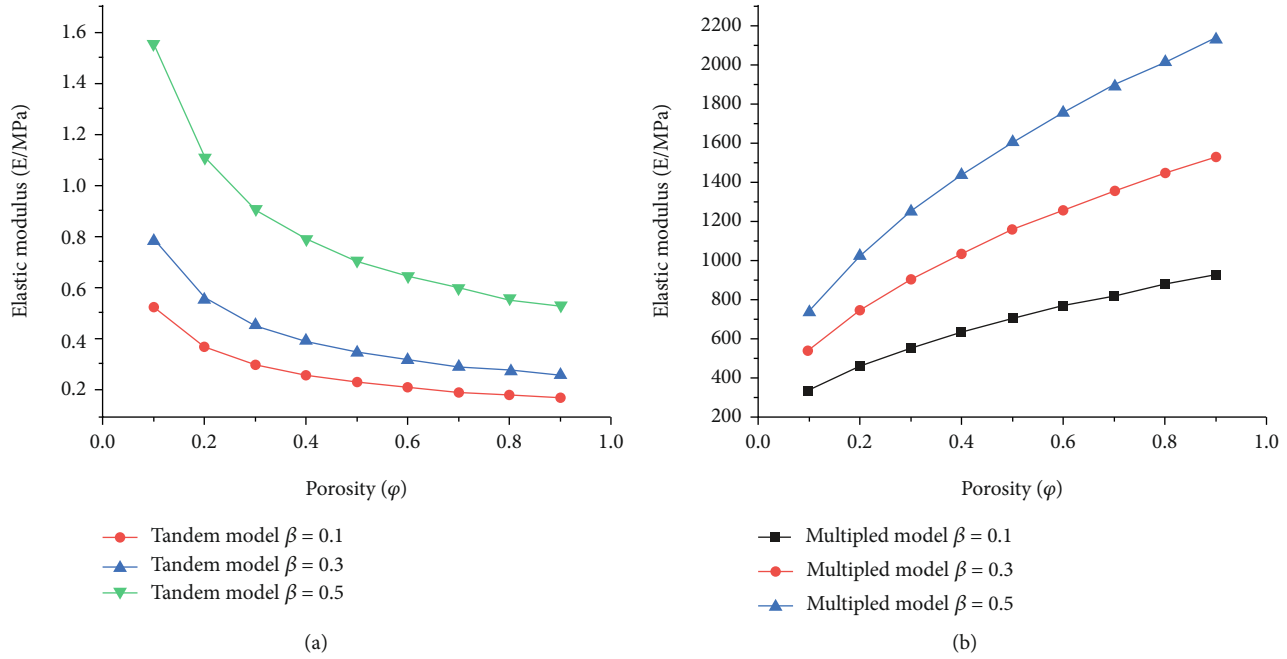

Figure 12: Relationship of elastic modulus E and porosity ϕ in simple weighted medial volume REV model under a different moisture content β.

respectively. The data in Figure 13 show that the proposed REV model's elastic modulus increases with the increasing number of tortuosity. On the other hand, its decreasing with the increasing number of stoma access distribution parameter is caused by the constant tortuosity.

Under the stoma access distribution parameter of $\eta = 0.5$, moisture content of $\beta = 0.3$, and ice percentage of $\alpha = 0.3$, the variation of elastic modulus E with tortuosity τ is plotted in Figure 14 with the porosity ϕ of 0.3, 0.5, and 0.7, respectively. The data in Figure 14 shows that the proposed REV model increases its elastic modulus with the increasing number of tortuosity when the constant porosity is maintained. This is because the increasing number of tortuosity leads to a higher elastic modulus. On the other hand, its increasing with the increasing number of porosity is caused by the constant tortuosity.

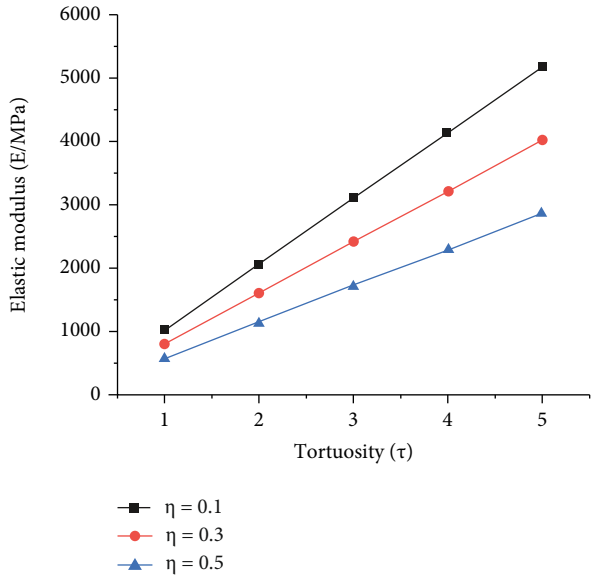

Figure 13: Relationship of elastic modulus E and tortuosity τ in fine weighted medial volume REV model under a different stoma access distribution parameter η.

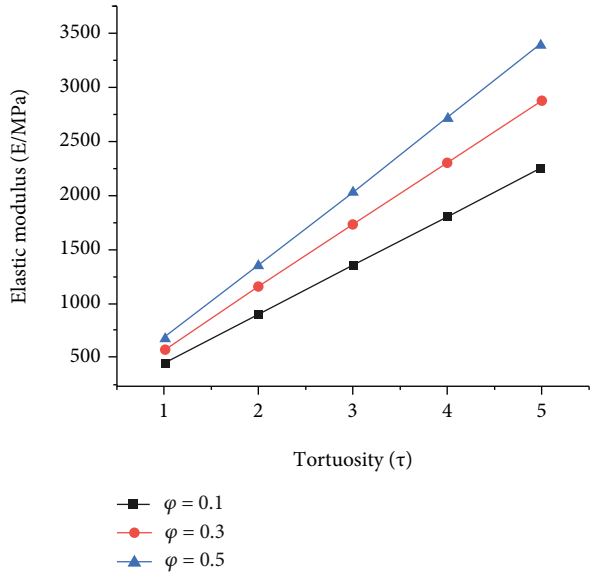

Figure 14: Relationship of elastic modulus E and tortuosity τ in fine weighted medial volume REV model under a different porosity ϕ.

Under the stoma access distribution parameter of $\eta = 0.5$, porosity of $\phi = 0.5$, and ice percentage of $\alpha = 0.3$, the variation of elastic modulus E with tortuosity τ is plotted in Figure 15 with the moisture content β of 0.1, 0.3, and 0.5, respectively. The data in Figure 15 shows that the proposed REV model's elastic modulus increases with the increasing number of moisture content when the constant tortuosity is maintained. This is because the increasing number of moisture content leads to a higher elastic modulus. On the other hand, its increasing with the increasing number of tortuosity is caused by the constant moisture content.

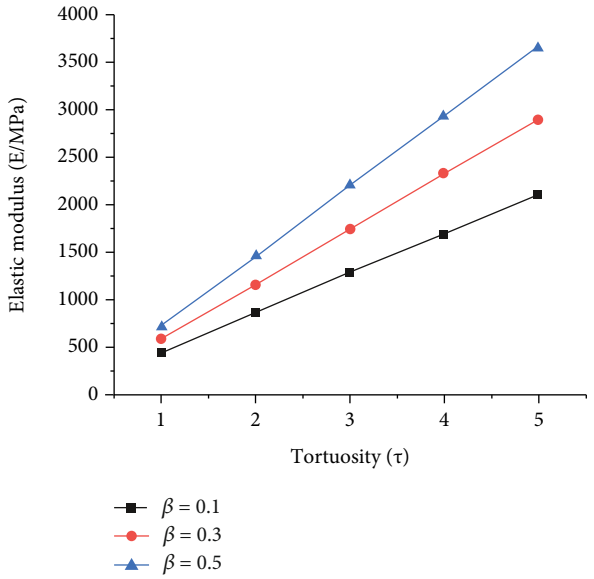

Figure 15: Relationship of elastic modulus E and tortuosity τ in the fine weighted medial volume REV model under a different moisture content β.

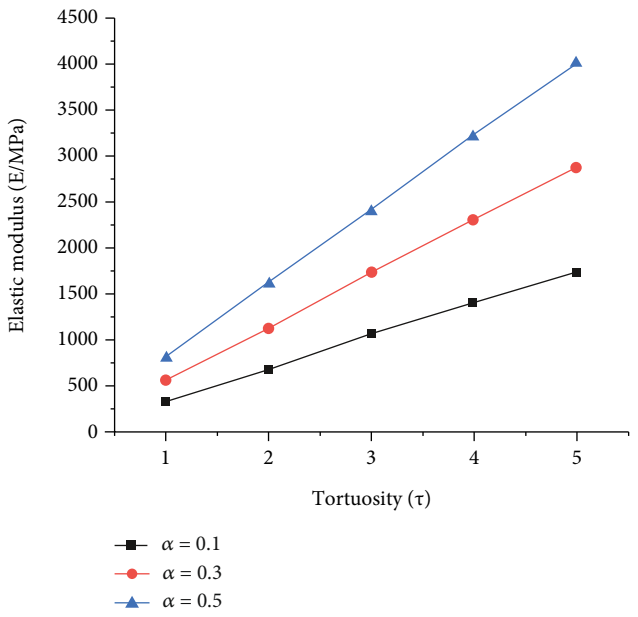

Figure 16: Relationship of elastic modulus E and tortuosity τ in the fine weighted medial volume REV model under a different ice percentage α.

Under the stoma access distribution parameter of $\eta = 0.5$, porosity of $\phi = 0.5$, and moisture content of $\beta = 0.3$, the variation of elastic modulus E with tortuosity τ is plotted in Figure 16 with the ice percentage α of 0.1, 0.3, and 0.5, respectively. The data in Figure 16 shows that the proposed REV model's elastic modulus increases with the increasing number of ice percentage when the constant tortuosity is maintained. This is because the increasing number of ice percentage leads to a higher elastic modulus. On the other hand, its increasing with the increasing number of tortuosity is caused by the constant ice percentage.

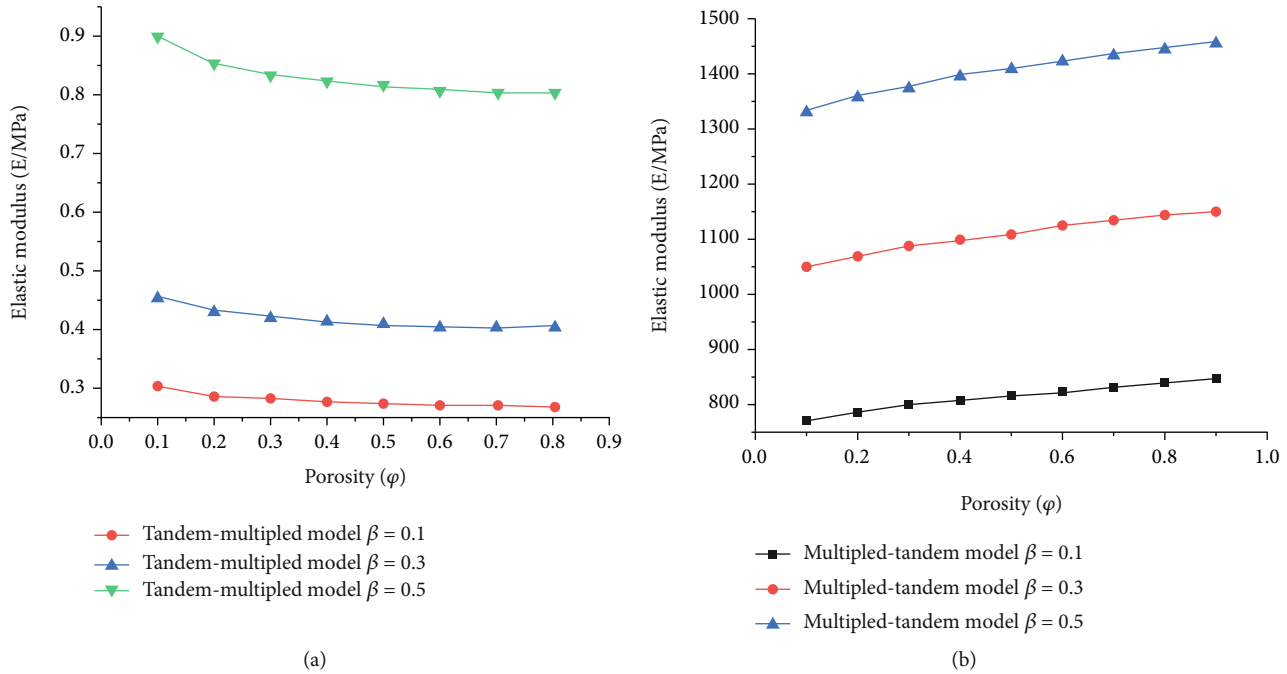

Figure 17: Relationship of elastic modulus E and porosity ϕ in the comprehensive REV model under a different moisture content β.

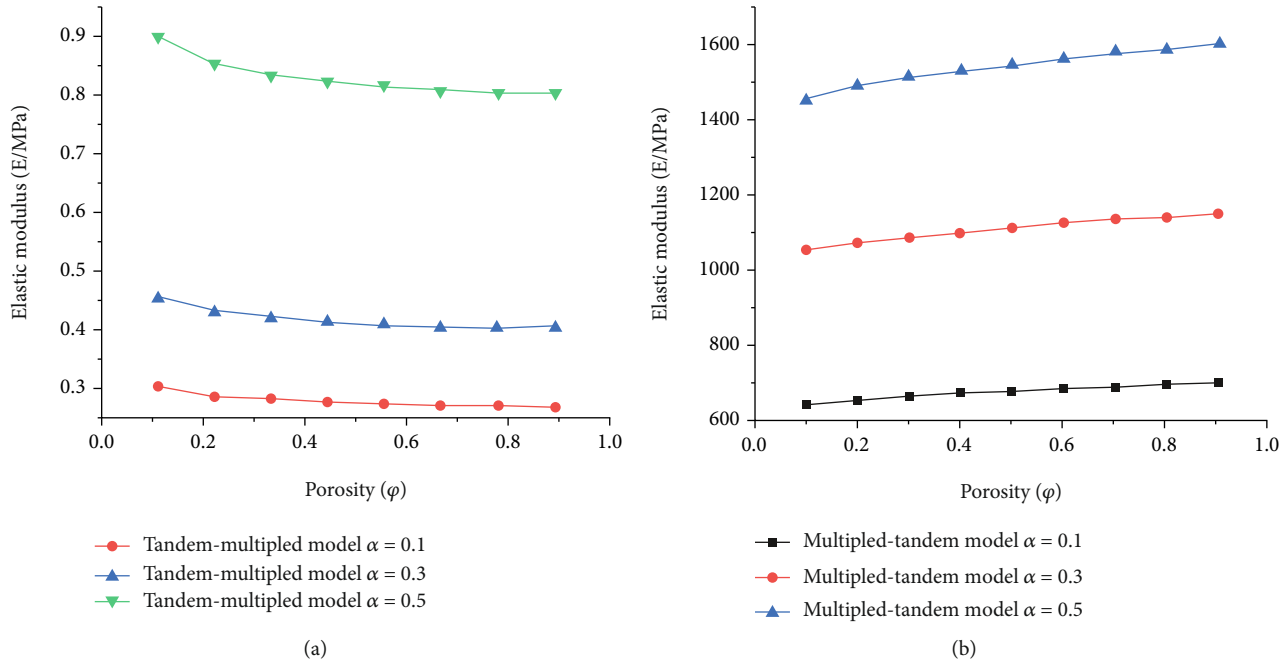

Figure 18: Relationship of elastic modulus E and porosity ϕ in a comprehensive REV model under a different ice percentage α.

4.4.3. Elastic Modulus Calculation by Comprehensive REV Model. Based on Equations (28) and (31), numerical simulation is performed on the elastic modulus by comprehensive model.

Under the ice percentage of $\alpha = 0.3$ and the moisture content β of 0.1, 0.3, and 0.5, respectively, the changes of elastic modulus E of the tandem-multipled model with the porosity ϕ are displayed in Figure 17(a), and the changes of elastic modulus E of the multipled-tandem model with the porosity ϕ is displayed in Figure 17(b). From this figure, it tends to be seen that, when the moisture content is constant, the elastic modulus obtained by the tandem-multipled model decreases with the increasing porosity, while that obtained by multipled-tandem model increases with the increasing porosity. Besides, when the porosity is constant, the elastic modulus obtained by the tandem-

multipled model and multipled-tandem model both increase with the increasing moisture content.

Under the moisture content of $\beta = 0.3$ and the ice percentage α of 0.1, 0.3, and 0.5, respectively, the changes of elastic modulus E of the tandem-multipled model with the porosity ϕ are displayed in Figure 18(a), and the changes of elastic modulus E of the multipled-tandem model with the porosity ϕ are displayed in Figure 18(b). From this figure, it tends to be seen that, when the ice percentage is constant, the elastic modulus obtained by the tandem-multipled model decreases with the increasing porosity, while that obtained by the multipled-tandem model increases with the increasing porosity. Besides, when the porosity is constant, the elastic modulus obtained by the tandem-multipled model and multipled-tandem model both increases with the increasing ice percentage.

5. Conclusions

In winter, the presence of water and others in the soil's stomas can cause a freeze-thawing phenomenon and a significant change in the material's elastic modulus. This paper presents an analysis of the multiple factors that affect the elastic modulus of unsaturated soil. The researchers used the data collected during the study to create models that takes into account the multiple composition and structure parameters of the soil. The results of the study were then used to perform a comparative analysis between the different models. The existing tests were used for relative confirmation and calculation analysis, and the accompanying conclusions are drawn:

(1) Assuming that the actual soil porous medium is a continuum, the properties of the soil's various components are analyzed and described according to the structure and composition of an unsaturated ice-free soil. The feasibility of incorporating the porosity and the permeability of the soil as a representative state variable are also examined

(2) According to the calculation formula deduced form physical model and taking sandy soil as example, numerical calculation is performed to study the variation trend of the elastic modulus under various parameters and factors (porosity, moisture content, ice percentage, and tortuosity). The model and numerical analysis show that, with the porosity (representing the extensive stoma distribution), the filling of fluid fixing medium becomes sufficient, the effective elastic modulus increases, the matrix continuity increases in space, the spatial dimension of the characterization unit increases, and the elastic modulus of multipled REV model is larger than that of tandem REV model as the porosity increases

(3) The work performed in this project is aimed at providing another way to the turn of events and development of frozen soil resources. It also contributes to the understanding of the various development rules and characteristics of permafrost. It also studies the effects of climate change on the establishment and maintenance of frozen structures

Data Availability

The data used to support the findings of this study are available from the corresponding author upon request.

Conflicts of Interest

No potential conflict of interest was reported by the authors.

References

[1] N. A. Tsytovich, *Mechanics of Frozen Soil*, St. Petersburg, USSR, 1973.

[2] E. Simonsen, V. C. Janoo, and U. Isacsson, "Resilient properties of unbound road materials during seasonal frost conditions," *Journal of Cold Regions Engineering*, vol. 16, no. 1, pp. 28–50, 2002.

[3] J. B. Burland, "Ninth Laurits Bjerrum Memorial Lecture: "small is beautiful"—the stiffness of soils at small strains," *Canadian Geotechnical Journal*, vol. 26, no. 4, pp. 499–516, 1989.

[4] W. Yu, Y. Lai, Y. Zhu et al., "In situ determination of mechanical properties of frozen soils with the pressuremeter," *Cold Regions Science and Technology*, vol. 34, no. 3, pp. 179–189, 2002.

[5] C. S. Yang, P. He, G. D. Cheng, S. P. Zhao, and Y. S. Deng, "Study of stress-strain relationships and strength characteristics of saturated saline frozen silty clay," *Rock and Soil Mechanics*, vol. 29, no. 12, pp. 3282–3286, 2008.

[6] V. R. Parameswaran and S. J. Jones, "Triaxial testing of frozen sand," *Journal of Glaciology*, vol. 27, no. 95, pp. 147–155, 1981.

[7] V. R. Parameswaran, "Deformation behaviour and strength of frozen sand," *Canadian Geotechnical Journal*, vol. 17, no. 1, pp. 74–88, 1980.

[8] R. A. Bragg and O. B. Andersland, "Strain rate, temperature, and sample size effects on compression and tensile properties of frozen sand," *Engineering Geology*, vol. 18, no. 1-4, pp. 35–46, 1981.

[9] X. Xu, Y. Wang, R. Bai, C. Fan, and S. Hua, "Comparative studies on mechanical behavior of frozen natural saline silty sand and frozen desalted silty sand," *Cold Regions Science and Technology*, vol. 132, pp. 81–88, 2016.

[10] J. C. Li, G. Y. Baladi, and O. B. Andersland, "Cyclic triaxial tests on frozen sand," *Engineering Geology*, vol. 13, no. 1-4, pp. 233–246, 1979.

[11] M. Christ and J. B. Park, "Ultrasonic technique as tool for determining physical and mechanical properties of frozen soils," *Cold Regions Science and Technology*, vol. 58, no. 3, pp. 136–142, 2009.

[12] X. Ling, Z. Zhu, F. Zhang et al., "Dynamic elastic modulus for frozen soil from the embankment on Beiluhe Basin along the Qinghai–Tibet Railway," *Cold Regions Science and Technology*, vol. 57, no. 1, pp. 7–12, 2009.

[13] D. Li and J. Fan, "A study of mechanical property of artificial frozen clay under dynamic load," *Advances in Civil Engineering*, vol. 2018, Article ID 5392641, 8 pages, 2018.

[14] J. Liu, Y. Cui, X. Liu, and D. Chang, "Dynamic characteristics of warm frozen soil under direct shear test-comparison with dynamic triaxial test," *Soil Dynamics and Earthquake Engineering*, vol. 133, article 106114, 2020.

[15] J. Bear, "Dynamics of fluids in porous media," *Soil Science*, vol. 120, no. 2, pp. 162-163, 1975.

[16] J. A. R. Borges, L. F. Pires, F. A. M. Cassaro et al., "X-ray microtomography analysis of representative elementary volume (REV) of soil morphological and geometrical properties," *Soil and Tillage Research*, vol. 182, pp. 112–122, 2018.

[17] J. Koestel, M. Larsbo, and N. Jarvis, "Scale and REV analyses for porosity and pore connectivity measures in undisturbed soil," *Geoderma*, vol. 366, article 114206, 2020.

[18] J. L. Gonzalez, E. L. de Faria, M. P. Albuquerque et al., "Representative elementary volume for NMR simulations based on X-ray microtomography of sedimentary rock," *Journal of Petroleum Science and Engineering*, vol. 166, pp. 906–912, 2018.

[19] H. Wu, Y. Yao, Y. Zhou, and F. Qiu, "Analyses of representative elementary volume for coal using X-ray μ-CT and FIB-SEM and its application in permeability predication model," *Fuel*, vol. 254, article 115563, 2019.

[20] O. M. O. De Araújo, K. V. Sharma, A. S. Machado et al., "Representative elementary volume in limestone sample," *Journal of Instrumentation*, vol. 13, no. 10, article C10003, 2018.

[21] L. C. S. M. Ozelim and A. L. B. Cavalcante, "Representative elementary volume determination for permeability and porosity using numerical three-dimensional experiments in microtomography data," *International Journal of Geomechanics*, vol. 18, no. 2, article 04017154, 2018.

[22] A. Puyguiraud, P. Gouze, and M. Dentz, "Is there a representative elementary volume for anomalous dispersion?," *Transport in Porous Media*, vol. 131, no. 2, pp. 767–778, 2020.

[23] S. Saraji and M. Piri, "The representative sample size in shale oil rocks and nano-scale characterization of transport properties," *International Journal of Coal Geology*, vol. 146, pp. 42–54, 2015.

[24] Q. Liu, X. B. Feng, Y. L. He, C. W. Lu, and Q. H. Gu, "Three-dimensional multiple-relaxation-time lattice Boltzmann models for single-phase and solid-liquid phase-change heat transfer in porous media at the REV scale," *Applied Thermal Engineering*, vol. 152, pp. 319–337, 2019.

[25] T. Liu and M. Wang, "Critical REV size of multiphase flow in porous media for upscaling by pore-scale modeling," *Transport in Porous Media*, vol. 36, pp. 1–22, 2021.

[26] Z. Niu, Z. Yang, Y. Luo et al., "The application of REV-LBM double mesh local refinement algorithm in porous media flow simulation," *Geofluids*, vol. 2022, Article ID 1082386, 12 pages, 2022.

[27] G. Kefayati, A. Tolooiyan, A. P. Bassom, and K. Vafai, "A mesoscopic model for thermal–solutal problems of power-law fluids through porous media," *Physics of Fluids*, vol. 33, no. 3, article 033114, 2021.

[28] Y. L. He, Q. Liu, Q. Li, and W. Q. Tao, "Lattice Boltzmann methods for single-phase and solid-liquid phase-change heat transfer in porous media: a review," *International Journal of Heat and Mass Transfer*, vol. 129, pp. 160–197, 2019.

[29] A. Singh, K. Regenauer-Lieb, S. D. C. Walsh, R. T. Armstrong, J. J. van Griethuysen, and P. Mostaghimi, "On representative elementary volumes of grayscale micro-CT images of porous media," *Geophysical Research Letters*, vol. 47, no. 15, article e2020GL088594, 2020.

[30] Q. Liu, H. Zhuang, Q. Wu, K. Zhao, and G. Chen, "Experimental study on dynamic modulus and damping ratio of rubber-sand mixtures over a wide strain range," *Journal of Earthquake and Tsunami*, vol. 16, no. 2, article 2140006, 2022.

[31] L. Qiu, Y. Zhu, D. Song et al., "Study on the nonlinear characteristics of EMR and AE during coal splitting tests," *Minerals*, vol. 12, no. 2, p. 108, 2022.

[32] H. Wu and G. Zhao, "Failure behavior of horseshoe-shaped tunnel in hard rock under high stress: phenomenon and mechanisms," *Transactions of Nonferrous Metals Society of China*, vol. 32, no. 2, pp. 639–656, 2022.

[33] M. He, Z. Zhang, J. Zhu, and N. Li, "Correlation between the constant mi of Hoek-Brown criterion and porosity of intact rock," *Rock Mechanics and Rock Engineering*, vol. 55, no. 2, pp. 923–936, 2022.

[34] X. L. Li, Z. Y. Cao, and Y. L. Xu, "Characteristics and trends of coal mine safety development," *Energy Sources, Part A: Recovery, Utilization, and Environmental Effects*, vol. 42, pp. 1–14, 2020.

[35] S. M. Liu, X. L. Li, D. K. Wang, and D. Zhang, "Investigations on the mechanism of the microstructural evolution of different coal ranks under liquid nitrogen cold soaking," *Energy Sources, Part A: Recovery, Utilization, and Environmental Effects*, vol. 42, pp. 1–17, 2020.

[36] X. L. Li, S. J. Chen, Q. M. Zhang, X. Gao, and F. Feng, "Research on theory, simulation and measurement of stress behavior under regenerated roof condition," *Geomechanics and Engineering*, vol. 26, no. 1, pp. 49–61, 2021.

[37] X. L. Li, S. J. Chen, S. M. Liu, and Z. H. Li, "AE waveform characteristics of rock mass under uniaxial loading based on Hilbert-Huang transform," *Journal of Central South University*, vol. 28, no. 6, pp. 1843–1856, 2021.

[38] X. L. Li, S. J. Chen, S. Wang, M. Zhao, and H. Liu, "Study on in situ stress distribution law of the deep mine taking Linyi Mining area as an example," *Advances in Materials Science and Engineering*, vol. 2021, Article ID 5594181, 11 pages, 2021.

[39] H. Y. Liu, B. Y. Zhang, X. L. Li et al., "Research on roof damage mechanism and control technology of gob-side entry retaining under close distance gob," *Engineering Failure Analysis*, vol. 138, no. 5, article 106331, 2022.

[40] Q. Han, Z. Wang, and R. Qin, "Thermal conductivity model analysis of unsaturated ice-containing soil," *Geoflfluids*, vol. 2022, article 3717705, 15 pages, 2022.

[41] X. Xu, Y. Lai, Y. Dong, and J. Qi, "Laboratory investigation on strength and deformation characteristics of ice-saturated frozen sandy soil," *Cold Regions Science and Technology*, vol. 69, no. 1, pp. 98–104, 2011.

[42] V. E. Panin, A. D. Korotaev, P. V. Makarov, and V. M. Kuznetsov, "Physical mesomechanics of materials," *Russian Physics Journal*, vol. 41, no. 9, pp. 856–884, 1998.

[43] A. Reuß, "Berechnung der fließgrenze von mischkristallen auf grund der plastizitätsbedingung für einkristalle," *ZAMM-Journal of Applied Mathematics and Mechanics/Zeitschrift für Angewandte Mathematik und Mechanik*, vol. 9, no. 1, pp. 49–58, 1929.

[44] X. Yuan, C. Wang, S. Zhao, and L. Zang, "Investigation on bulk elastic modulus of air and liquid mixing fluid," *Journal of Mechanical Engineering*, vol. 55, no. 10, pp. 226–232, 2019.

[45] W. Voigt, "Uber Die Beziehung Zwischen Den Beiden Elastizitiitskonstanten Isotroper Krper," *Wied Ann*, vol. 38, pp. 573–587, 1889.

[46] W. Y. Jiang, *Study on Strength Characteristics and Constitutive Model of Frozen Silty Clay*, Nanjing Forestry University, Nanjing China, 2017.

[47] Z. Z. Wang, S. Y. Mu, Y. H. Niu, L. J. Chen, J. Liu, and X. D. Liu, "Predictions of elastic constants and strength of transverse isotropic frozen soil," *Rock and Soil Mechanics*, vol. 29, no. 1, pp. 475–480, 2008.

[48] D. F. Elger, B. A. LeBret, C. T. Crowe, and J. A. Roberson, *Engineering Fluid Mechanics*, John Wiley and Sons, Idaho, USA, 2020.